JOURNAL OF MATERIALS SCIENCE 32 (1997) 6633–6638

Ultrasonic through-transmission method of evaluating the modulus of elasticity of Al_2O_3–ZrO_2 composite

TAN KHA SHEN, P. HING
School of Applied Science, Nanyang Technological University, Singapore

The elastic properties of Al_2O_3–ZrO_2 composite were determined from ultrasonic velocity measurements, and were found to be dependent upon the amount of ZrO_2 phase, the compacting pressure of the green ceramic and sintering time. The velocity in the Al_2O_3–ZrO_2 composite increased to a maximum for about 3 wt% unstabilized ZrO_2 dispersed in Al_2O_3. The velocity decreased monotonically thereafter. The increase in moduli, as shown by an increase in velocity, has been attributed to phase transformation of the unstabilized ZrO_2 from tetragonal to a monoclinic phase, which presumably leads to a toughening and strengthening effect, and also due to the action of ZrO_2 in stopping grain growth of Al_2O_3 during densification. The excessive shear strain, induced by the tetragonal→monoclinic transformation phase, with greater than 50 wt % ZrO_2 content, caused microcracks to appear in the composite. This reduced the elastic moduli of the composite. It was found that the composition dependence of the elastic moduli lie outside the theoretical bound of Voigt and Reuss for the elastic moduli of two-phase materials, and that by increasing the compacting pressure, an improvement in the elastic moduli of the sintered composite occurred irrespective of ZrO_2 content. The thermal expansion of the composites showed no appreciable change with addition of zirconia up to 5 wt % ZrO_2. However, dimensional changes due to phase transformation particularly with high zirconia content have been established.

1. Introduction

A small addition of ZrO_2 to alumina has been reported to enhance the mechanical properties of alumina–zirconia composites [1–4]. The improvement in properties has been linked to the polymorphic transformation of ZrO_2 from the tetragonal to the monoclinic phase ($t \rightarrow m$) which is accompanied by a volume expansion of about 3%–5%. An example is ZrO_2-toughened Al_2O_3 (ZTA) [1, 2] which exhibit high hardness and toughness compared to Al_2O_3. The ZrO_2 in ZTA is also reported to hinder grain growth of Al_2O_3 [5–7]. This apparently improves the microstructure of ZTA. Two of the mechanisms by which toughness and hardness are achieved in Al_2O_3–ZrO_2 composite, are attributed to stress-induced transformation toughening [8], and resistance to crack propagation by the ZrO_2 particles [8, 9]. These mechanisms are also responsible for the increase in the elastic moduli for small ZrO_2 content. At high ZrO_2 content, the elastic moduli of the composite decrease markedly. One of the methods of measuring the elastic moduli is by measuring the speed of ultrasound through the composite. This measures the dynamic elastic moduli. The present work deals primarily with the processing and the determination of the moduli of elasticity of sintered Al_2O_3–ZrO_2 composites.

2. Experimental procedure

Anhydrous γ-Tonerde Al_2O_3 (Merck Art. 1095) was milled for 48 h and the unstabilized ZrO_2 (Fluka Chemika 96594) was milled for 68 h. The BET surface area of the milled powders was measured using the Micrometrics ASAP 2000. Both the alumina and zirconia were thoroughly mixed with 4 wt % polyvinyl alcohol. The slurries were dried and the powders passed through a 180 μm mesh stainless steel sieve. ZrO_2 was mechanically mixed with the Al_2O_3 to obtain a homogeneous mixture. Each batch of powder, with different wt % ZrO_2, was compressed uniaxially into 20 mm diameter pellets at room temperature. Compacting pressures of 122, 163 and 244 MPa were used. The bulk densities of the green and sintered pellets were obtained from the mass and the dimensions. The samples were dried in the oven at 70 °C in air for 6 h and sintered in air at 1550 °C for 2 h.

The compression and shear velocities of each sintered sample were measured, using the through-transmission method, with a thin water-soluble gel to couple the probes to the sample. The apparatus is shown in Fig. 1. Matched compressional wave probes of diameter 0.635 cm (0.25 in) with a nominal transmitting frequency of 5 MHz, and shear wave probes of diameter 1.27 cm (0.5 in) with a nominal transmitting frequency of 2.5 MHz, were used. The coupling gel

0022–2461

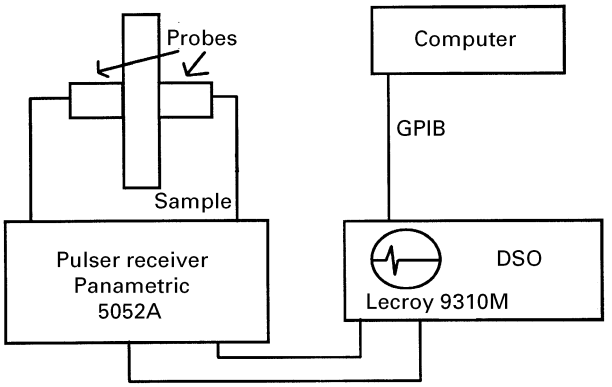

Figure 1 Schematic diagram of time of flight of ultrasonic pulse through the sample.

does not affect the physical or chemical properties of the samples. When using any couplant to obtain an acceptable acoustic contact between probes and sample surface, care must be taken to use only a very thin amount of the couplant, because the porous nature of the ceramic would absorb any excess couplant, which can change the wave speed through the composite [10]. A piece of the sintered sample was cut with a diamond-impregnated wheel. The cross-section of the cut sample was polished down to about 3 μm finish. All the polished samples were thermally etched in air at 1250 °C for 60 min. The microstructures were observed optically and by scanning electron microscopy (SEM).

The thermal expansion of the ZrO_2–Al_2O_3 composites up to 1500 °C was also measured using a Netzsch. The samples for dilatometry were cut from the same samples used in the ultrasonic velocity measurements.

3. Results and discussion

3.1. Compressional and shear-wave velocity measurements

The compressional and shear velocities can be calculated by measuring the transit time of the ultrasonic pulse through the thickness of the sample.

The measured compressional and shear-wave velocities plotted against wt % ZrO_2 are shown in Fig. 2. It can be seen that the compressional and shear velocities increase with greater compacting pressure used to form the green ceramic compact. The velocities also increase with ZrO_2 with a maximum at about 3 wt %.

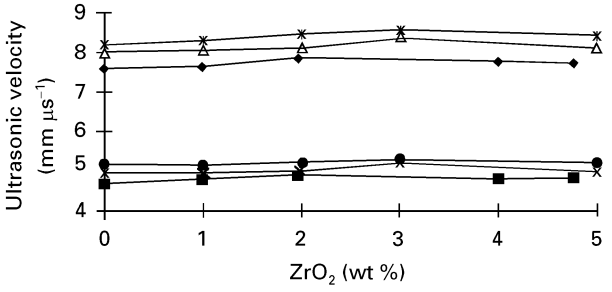

Figure 2 (♦, △, ∗) Compressional and (■, ×, ●) shear velocities at compacting pressure of (♦, ■) 122 MPa, (△, ×) 163 MPa and (∗, ●) 244 MPa. The shear velocities are slightly more than half the compressional velocities.

3.2. Dependence of elastic properties on ZrO_2

For an isotropic polycrystalline material, the ultrasonic compressional and shear velocities are related to the elastic moduli by the equations [11–13]

$$G = V_s^2 \rho \tag{1}$$

$$K = \frac{\rho(3V_c^2 - 4V_s^2)}{3} \tag{2}$$

$$E = \frac{V_s^2 \rho(3V_c^2 - 4V_s^2)}{V_c^2 - V_s^2} \tag{3}$$

$$\sigma = \frac{V_c^2 - 2V_s^2}{2(V_c^2 - V_s^2)} \tag{4}$$

where G is the shear modulus (GPa), K is the bulk modulus (GPa), E is the Young's modulus (GPa), σ is Poisson's ratio, V_c is the compressional velocity (mm μs^{-1}), V_s is the shear velocity (mm μs^{-1}) and ρ is the bulk density of the sample (kg m^{-3}).

The calculated elastic moduli and Poisson's ratio were plotted against wt % ZrO_2, as shown in Figs 3–6

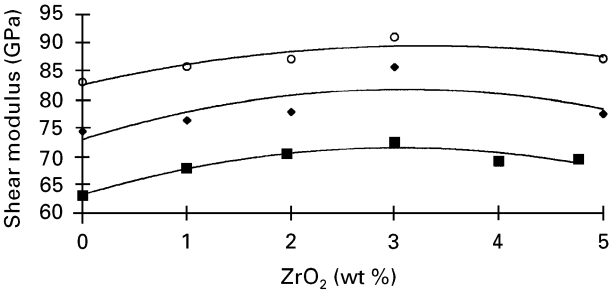

Figure 3 Shear modulus at compacting pressure of ■ 122 MPa, (♦) 163 MPa and (○) 244 MPa.

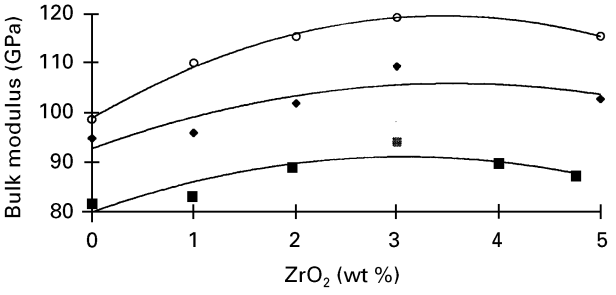

Figure 4 Bulk modulus at compacting pressure of (■) 122 MPa, (♦) 163 MPa and (○) 244 MPa.

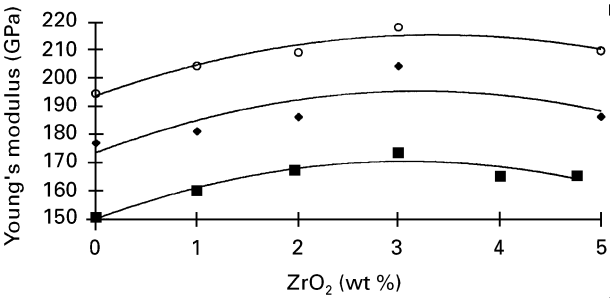

Figure 5 Young's modulus at compacting pressure of (■) 122 MPa, (♦) 163 MPa and (○) 244 MPa.

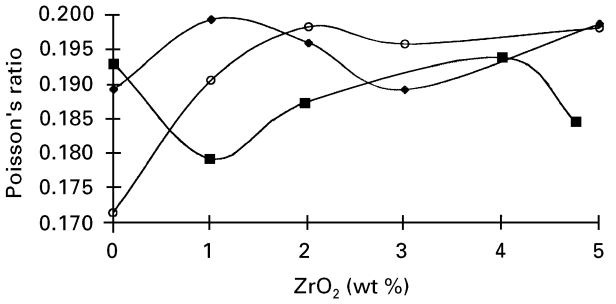

Figure 6 Poisson's ratio at compacting pressure of (■) 122 MPa, (♦) 163 MPa and (○) 244 MPa.

using Equations 1–4, respectively. From the graphs of the elastic moduli (Figs 3–5), it can be seen that the moduli increase with greater compacting pressure. Doubling the compacting pressure from 122 MPa to 244 MPa causes G, K and E for pure Al_2O_3 to increase by about 34%, 23% and 30%, respectively. Irrespective of compacting pressure, the moduli also increase, with higher wt % ZrO_2, up to a maximum at about 3 wt % ZrO_2. The average increase in G, K and E, from 0 wt % to 3 wt %, is about 14%, 18% and 15%, respectively. At 3 wt % ZrO_2, the increase in G, K and E is about 25%, 27% and 25%, respectively, for a doubling in compacting pressure from 122 MPa to 244 MPa.

From Fig. 6, the Poisson's ratio, at room temperature, varies from greater than 0.17 to less than about 0.2, indicating a brittle and hard composite as compared with normal metal alloy which has a ratio of 0.3 and above. It might be envisaged that such composites would also become plastic ($\sigma = 0.5$) either under extremely high hydrostatic pressure at room temperature (e.g. [14]) or under an extended time tensile load at high temperature ($> 1500\,^{\circ}C$) [15].

The compositional dependence of the elastic moduli might be compared with the theoretical bounds of Voigt and Reuss [16] as given below

Voigt model (upper bound)

$$E_v = V_2 E_2 + (1 - V_2) E_2 \quad (5)$$

Reuss model (lower bound)

$$E_r = \frac{E_2 E_1}{E_1 V_2 + E_2(1 - V_2)} \quad (6)$$

where E_1 and E_2 are the elastic moduli of the two phases in the composite, in this case that of Al_2O_3 and ZrO_2, respectively, V_2 is the volume fraction of phase with elastic modulus E_2. The Voigt model assumes that the strain in each phase is the same, while the Reuss model assumes that the stress in each phase is the same. Hashin and Shtrikman [17] derived a narrower bound than that given by Equations 5 and 6. Nevertheless, we will use only the Voigt and Reuss models, as our results show that the data lie outside either bound. The modulus as determined from measurement for 0 and 100 wt % ZrO_2, at a particular compacting pressure, is taken as E_1 and E_2, respectively. Table I shows the determined elastic moduli for Al_2O_3 and ZrO_2 for compacting pressure at 122, 163 and 244 MPa.

TABLE I Young's modulus of Al_2O_3 and ZrO_2

Compacting pressure (MPa)	E_1 (GPa) Al_2O_3	E_2 (GPa) ZrO_2
122	150.38	124.90
163	176.74	131.35
244	194.52	170.00

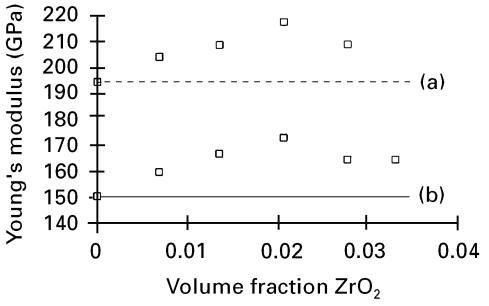

Figure 7 (a) Voigt and (b) Reuss bounds for different ZrO_2 contents at (– – –) 122 MPa and (——) 244 MPa, (□) Experimental data.

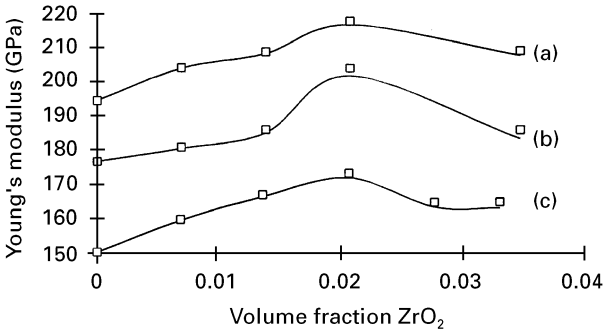

Figure 8 Modified Voigt and Reuss bounds at (a) 122 MPa, (b) 163 MPa and (c) 244 MPa. (□) Experimental data.

Figs 7 and 8 show the Voigt and Reuss bound of the Young's modulus for various wt % ZrO_2. It can be seen that the experimental data fall outside these bounds. The Voigt and Reuss bounds fall along the same line, i.e. the bounds are very narrow due to the small difference in E_1 and E_2. The bounds assume there are no interactions between the two phases to influence the upper and lower bound moduli. Various studies on the toughness and strength of alumina–zirconia ceramics show that ZrO_2 influences the strength and toughness of the alumina–zirconia system. The mechanisms by which ZrO_2 enhanced the mechanical properties, are stress-induced transformation toughening and resistance to crack propagation by the ZrO_2 particles as mentioned in the introduction. This is accomplished by its polymorphic transformation from the tetragonal to the monoclinic phase ($t \rightarrow m$) which is accompanied by a volume expansion of about 3%–5%. ZrO_2 also prevents large grain growth of Al_2O_3 [7, 18], thereby increasing the overall strength of the composite. Therefore, the modulus for the first phase, E_1, is influenced by ZrO_2 particles dispersed in the composite. If the bound is modified such that E_1 is taken as the Young's modulus from

ultrasonic determination as shown in Fig. 5, an empirical fit can be achieved with the experimental data. The "modified" Voigt and Reuss bounds are shown in Fig. 9. A full plot from 0–100 wt % ZrO_2 is shown in Fig. 8. The bounds were found to fit the experimental data up to about 25 wt % (0.2 volume fraction) ZrO_2 and deviate from the experimental data at greater than 25 wt % ZrO_2. Pores and microcracks that form in ceramics during fabrication [19–21] are particularly evident at ZrO_2 content greater than 25 wt %.

The influence of pores and microcracks on the composite does not play a significant part right up to 25 wt % ZrO_2, particularly if a stabilized agent is used, e.g. yttria [18]. The thermal expansion of the sintered composites is shown in Figs 10 and 11 for composites compacted at 122 and 244 MPa. The wriggling curves at low temperature, up to about 500 °C, were due to the measurement and heater control of the dilatometer system. This only happens at low temperature. As observed from Fig. 10, there is no significant change in the rate of expansion with

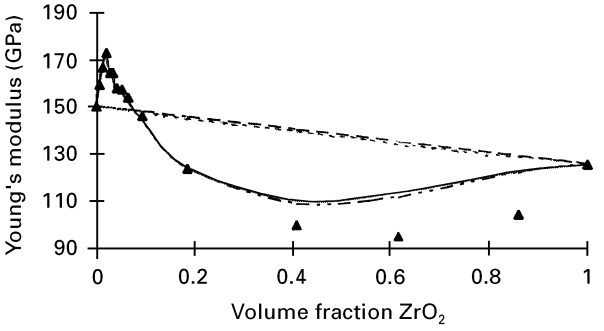

Figure 9 Modified Voigt and Reuss for the volume fraction ZrO_2 from 0–1 for a compacting pressure of 122 MPa. (– – –) Reuss, (— — —) Voigt, (— · —) modified Reuss, (——) modified Voigt, (▲) experimental data.

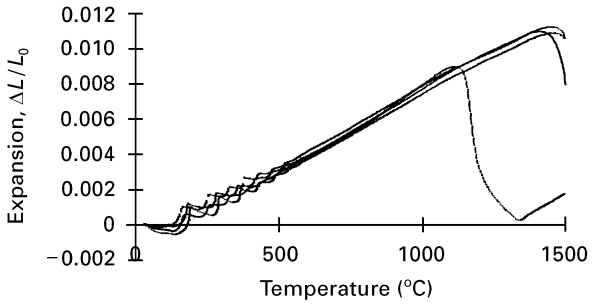

Figure 10 Dilatometer measurement of Al_2O_3–ZrO_2 composites at a compacting pressure of 244 MPa: (——) 0 wt %, (– – –) 3 wt %, (- - -) 5 wt %, (— · —) 100 wt %.

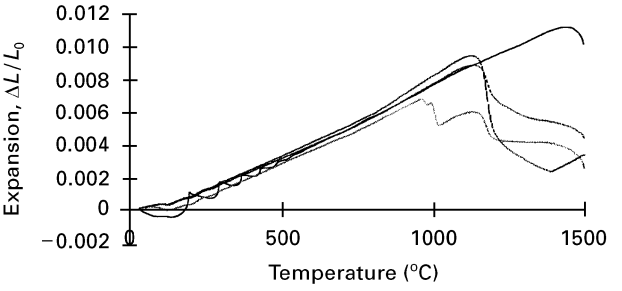

Figure 11 Dilatometer measurement of Al_2O_3–ZrO_2 composites at a compacting pressure of 122 MPa: (——) 2 wt %, (– – –) 50 wt %, (- - -) 70 wt %, (— · —) 90 wt %.

TABLE II Thermal expansion of Al_2O_3–ZrO_2 at 800 °C

ZrO_2 (wt %)	Compacting pressure (MPa)	Expansion coefficient (10^{-6} °C^{-1})
0	244	11.29
2	122	8.741
3	244	8.784
5	244	8.852
50	122	8.279
70	122	8.770
90	122	8.756
100	244	7.555

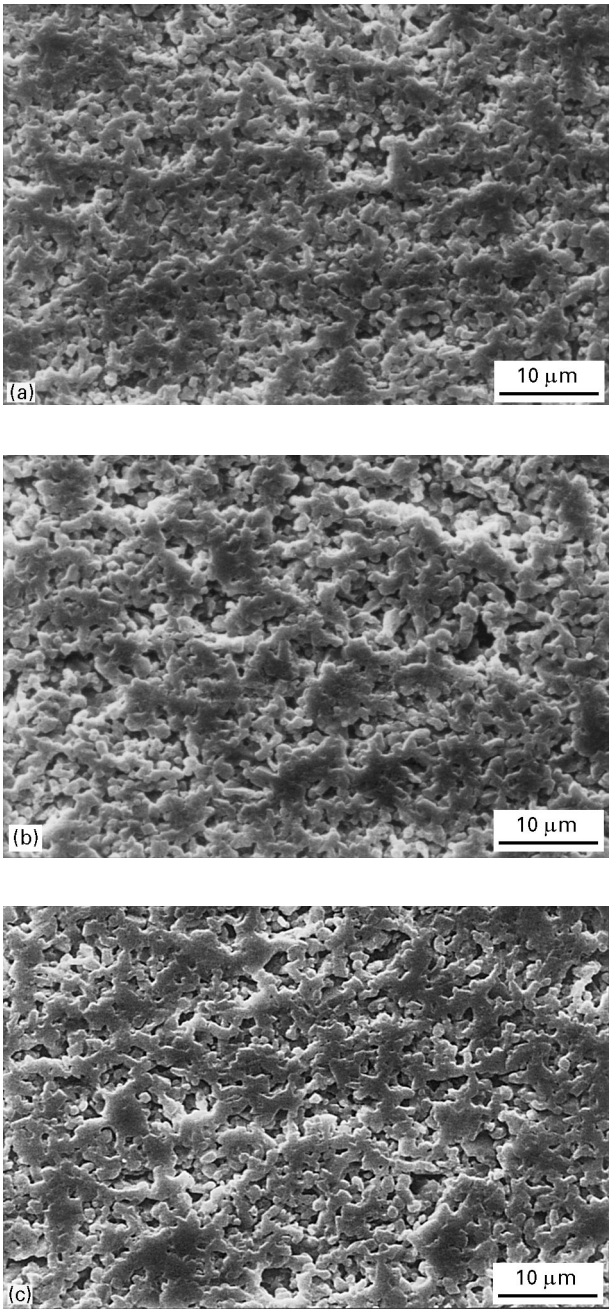

Figure 12 Micrographs of the polished surface of (a) pure alumina, (b) with 2 wt % ZrO_2, (c) with 3 wt % ZrO_2, (d) with 5 wt % ZrO_2 and (e) 100 % ZrO_2. The composites were sintered in air for 1550 °C for 2 h. The green samples were compacted at 244 MPa.

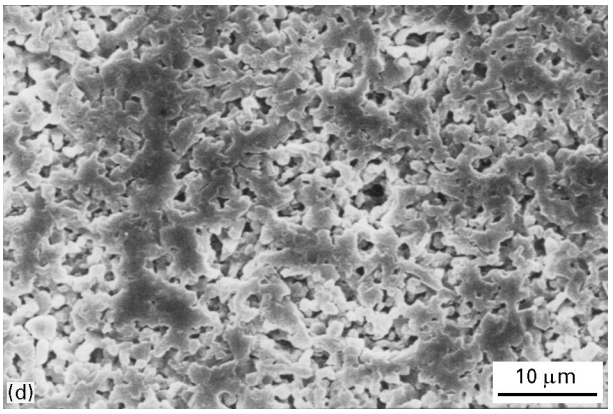

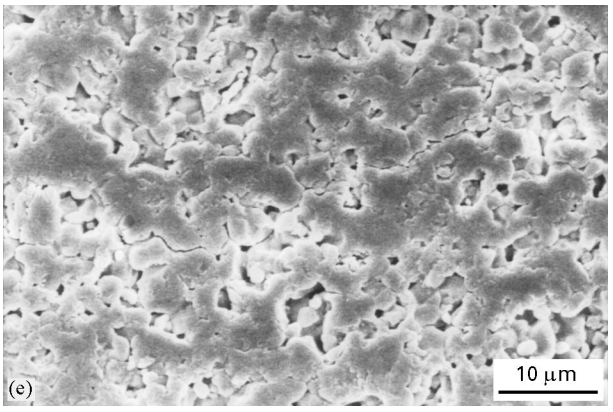

Figure 12 Continued.

temperature for 0–5 wt % ZrO_2. The expansion coefficients at 800 °C for Figs 10 and 11 are shown in Table II. At higher wt % ZrO_2, there is a transition at about 1100 °C due to polymorphic transformation of ZrO_2 from the monoclinic to the tetragonal phase. This transformation is reversible. For 50 wt % ZrO_2, there is also an unspecific change between 900 and 1100 °C.

Fig. 12a–e show scanning electron micrographs of polished surfaces of the composites, sintered in air for 2 h, containing 0, 2, 3, 5 and 100 wt % ZrO_2. The green composites were compacted at 244 MPa. Fig. 13a–c show micrographs of polished surfaces of composites, sintered in air for 2 h, containing 50, 70, and 90 wt % ZrO_2. The green composites were compacted at 122 MPa. The alumina and zirconia grains could not be distinguished very well without imaging with backscattered electrons. However, XRD analysis shows that all the zirconia grains were of the monoclinic phase (baddeleyite) while the alumina grains were mostly alpha-corundum. Other workers identified the zirconia grains as small round and irregularly shaped. The zirconia crystallites were enmeshed intergranularly as well as intragranularly among the alumina grains [7, 18].

Examination of the microstructures of samples containing 0–5 wt % ZrO_2 (compacted at 244 MPa) indicates that a small addition of zirconia improved the sinterability of alumina (Fig. 12a–c). The sintered density has, in fact, increased from 82% to 85.5% theoretical density. At around 50 wt % ZrO_2, the grain growth is different (Fig. 13a). The microstructure is

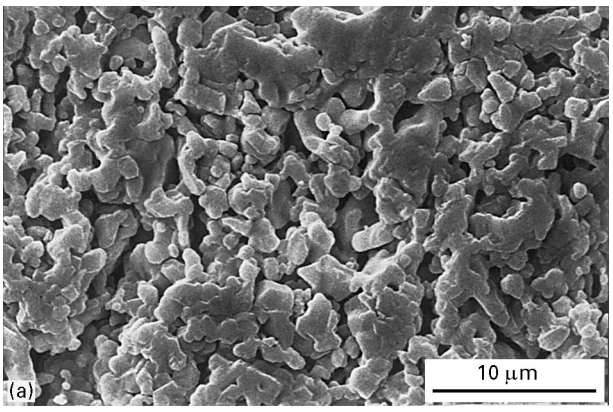

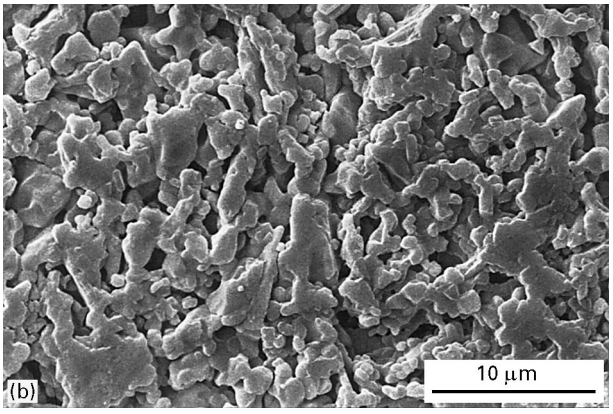

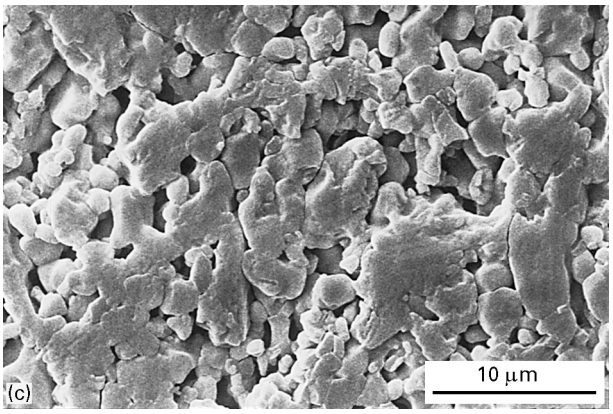

Figure 13 Micrograph of the polished surface of three Al_2O_3–ZrO_2 samples with (a) 50, (b) 70 and (c) 90 wt % ZrO_2. The composites were sintered in air at 1500 °C for 2 h. The green samples were compacted at 122 MPa.

quite porous and the sinterability is poor. Improved sintering behaviour, however, is observed from 70 wt % ZrO_2 upwards (Fig. 13b, c and Fig. 12e), although residual porosity and microcracks can be easily seen. Samples containing only zirconia were found to have sintered significantly with a density of about 85% theoretical. The increase in moduli with small addition of ZrO_2 is believed to be due to the control of alumina grain size, size distribution and grain shape by ZrO_2 [8] and the subsequent reduction in moduli is attributed to increase in microcracks and flaw size [22]. Increase in moduli at high ZrO_2 (above 70 wt %) is due to a decrease in volume fraction of porosity, which compensates for an increase in microcracks.

4. Conclusion

The moduli of a material have been determined by measuring the compression and shear velocities through the material and the associated bulk density. The moduli of the Al_2O_3–ZrO_2 composite can be enhanced by (1) increasing the compacting pressure of the green composite, thereby reducing the pore volume fraction and increasing its bulk density, and (2) with addition of < 5 wt % unstabilized ZrO_2. Defects, such as microcracks and porosity, cause the velocity, and hence the modulus, through such materials to be lower than its defect-free counterpart. The theoretical bounds of Voigt and Reuss are found to fit the experimental data of the Young's modulus up to 25 wt % ZrO_2 if the modulus of the composite is substituted for the modulus of the first phase (filler matrix) in the theoretical bounds.

Acknowledgement

The authors thank Dr N. Guo, MPE, and technicians in SAS and MPE, Nanyang Technological University, for their assistance in this study. The authors acknowledge the support of Professor Fong Hock Sun, Head of Materials Engineering, in this investigation.

References

1. N. CLAUSSEN, *J. Amer. Ceram. Soc.* **59** (1976).
2. *Idem*, *ibid.* **61** (1978) 85.
3. S. HORI and R. KURITA, *Adv. Ceram. Sci. Technol. Zirconia III* **24A** (1988) 423.
4. T. S. YEN and J. K. GUO, *ibid.* **24B** (1988) 573.
5. F. F. LANGE and M.M. HIRLINGER, *J. Amer. Ceram. Soc.* **67** (1984) 164.
6. S. HORI, R. KURITA, M. YOSHIMURA and S. SOMIYA, *J. Mater. Sci. Lett.* **4** (1985) 1067.
7. P. Y. DALVI and D. D. UPADHYAYA, *Trans. Ind. Ceram. Soc.* **49** (2) (1990) 21.
8. J. WANG and R. STEVENS, *J. Mater. Sci.* **24** (1989) 3421.
9. A. G. EVANS and A. H. HEUER, *J. Amer. Ceram. Soc.* **63** (5) (1980) 241.
10. F. VODAK, *Acta Mechan.* **39** (1981) 37.
11. K. S. TAN, R. ROUND and B. BRIDGE, *Br. Ceram. Trans. J.* **88** (4) (1989) 138.
12. R. HALMSHAW, "Non-destructive testing" (Edward Arnold, 1987) pp. 112–13.
13. J. BLITZ, "Elements of acoustics" (Butterworths, 1976).
14. P. W. BRIDGEMAN, "Studies in large plastic flow" (McGraw –Hill, New York, 1952).
15. E. RYSHKEWITCH and D. W. RICHERSON, "Oxide Ceramics" (General Ceramics, New York, 1985) pp. 143–53.
16. W. D. KINGERY, H. K. BOWEN and R. H. UHLMANN, "Introduction to ceramics", 2nd Edn (Wiley, 1975) pp. 773–7.
17. Z. HASHIN and S. SHTRIKMAN, *J. Mech. Phys. Solids* **11** (1963) 127.
18. B. L. MITRA, N. C. BISWAS and P. S. AGGARWAL, *Bull. Mater. Sci.* **15** (2) (1992) 131.
19. G. DE PORTU and P. VINCENZINI, *Short Commun.* **5** (1979) 165.
20. *Idem*, *Ceram. Int.* **6** (1980) 129.
21. G. DE PORTU, C. FIORI and O. SBAIRERO, *Adv. Ceram.* **24B** (1988) 1063.
22. D. J. ROTH, D. B. STANG, S. M. SWICKARD, M. R. DEGUIRE and L. E. DOLHERT, *Mater. Eval.* July (1991) 883.

Received 15 June
and accepted 20 November 1995